Functional connectivity among brain regions affected in Alzheimer's disease is associated with CSF TNF-alpha in APOE4 carriers

Contreras, Joey Annette; Aslanyan, Vahan; Sweeney, Melanie D.; Sanders, Lianne M. J.; Sagare, Abhay P.; Zlokovic, Berislav; Toga, Arthur W.; Han, S. Duke; Morris, John C.; Fagan, Anne

Published in:
Neurobiology of Aging

DOI:
10.1016/j.neurobiolaging.2019.10.013

Publication date:
2020

Neurobiology of Aging 86 (2020) 112–122

Contents lists available at ScienceDirect

Neurobiology of Aging

journal homepage: www.elsevier.com/locate/neuaging

Functional connectivity among brain regions affected in Alzheimer's disease is associated with CSF TNF-α in *APOE*4 carriers

Joey Annette Contreras [a], Vahan Aslanyan [a], Melanie D. Sweeney [b], Lianne M.J. Sanders [a,c], Abhay P. Sagare [b], Berislav V. Zlokovic [b], Arthur W. Toga [a], S. Duke Han [d], John C. Morris [e,f], Anne Fagan [e,f], Parinaz Massoumzadeh [e], Tammie L. Benzinger [e,g], Judy Pa [a,*]

[a] Mark and Mary Stevens Neuroimaging and Informatics Institute, University of Southern California, Los Angeles, CA, USA
[b] Zilkha Neurogenetic Institute, University of Southern California, Los Angeles, CA, USA
[c] Department of Human Movement Sciences, University Medical Center Groningen, University of Groningen, Groningen, the Netherlands
[d] Family Medicine, Neurology, Psychology, and Gerontology, Keck School of Medicine of the University of Southern California, Los Angeles, CA, USA
[e] Knight Alzheimer's Disease Research Center, Washington University, St. Louis, MO, USA
[f] Department of Neurology, Washington University, St Louis, MO, USA
[g] Department of Radiology and Neurological Surgery, Washington University, St. Louis, MO, USA

ARTICLE INFO

Article history:
Received 22 June 2019
Received in revised form 20 September 2019
Accepted 22 October 2019
Available online 5 November 2019

Keywords:
Alzheimer's disease
Resting-state fMRI
Neuroinflammation
TNF-Alpha
*APOE*4 carriers
Nucleus accumbens
Functional connectivity

ABSTRACT

It is now recognized that understanding how neuroinflammation affects brain function may provide new insights into Alzheimer's pathophysiology. Tumor necrosis factor (TNF)-α, an inflammatory cytokine marker, has been implicated in Alzheimer's disease (AD), as it can impair neuronal function through suppression of long-term potentiation. Our study investigated the relationship between cerebrospinal fluid TNF-α and functional connectivity (FC) in a cohort of 64 older adults (μ age = 69.76 years; 30 cognitively normal, 34 mild AD). Higher cerebrospinal fluid TNF-α levels were associated with lower FC among brain regions important for high-level decision-making, inhibitory control, and memory. This effect was moderated by apolipoprotein E-ε4 (*APOE*4) status. Graph theory metrics revealed there were significant differences between *APOE*4 carriers at the node level, and by diagnosis at the network level suggesting global brain network dysfunction in participants with AD. These findings suggest proinflammatory mechanisms may contribute to reduced FC in regions important for high-level cognition. Future studies are needed to understand the role of inflammation on brain function and clinical progression, especially in *APOE*4 carriers.

1. Introduction

Beta-amyloid and neurofibrillary tangles are the hallmark features of Alzheimer's pathology. However, it is increasingly recognized that other pathological insults, such as neuroinflammation, may be involved in the Alzheimer's cascade (Ardura-Fabregat et al., 2017; Bronzuoli et al., 2016; Sweeney et al., 2015). For instance, activation of neuroinflammatory systems is elevated in Alzheimer's disease (AD) relative to normal aging (Breunig et al., 2013; Heneka et al., 2015). Microglia, astrocytes, and even neurons have been shown to directly react and contribute to chronic neuroinflammatory responses in AD. It has been suggested that astrocyte and microglial activation may be an early event in the pathophysiology of AD, occurring even in the absence of focal amyloid-β (Aβ) deposition (Dudal et al., 2004).

Apolipoprotein E-ε4 (*APOE*4), a major genetic risk factor for late-onset AD, provides a unique opportunity to evaluate AD risk before the onset of clinical symptoms. *APOE* is an important modulator of immune responses, as evidenced by greater immune activation in mice lacking *APOE* (Liu et al., 2015). Particularly, *APOE*4 has been shown to promote the strongest proinflammatory effects in mouse models (Guo et al., 2004; Vitek et al., 2009) with additional evidence that *APOE*4 transgenic mice show increased susceptibility to inflammation compared with *APOE*2 and *APOE*3 mice (den Hartigh et al., 2012; Rodriguez et al., 2014; Zhu et al., 2012).

The induction of a microglial neuroinflammatory response results in the release of various inflammatory mediators including an array of neurotoxic cytokines (Akiyama et al., 2000; Tan et al., 2002).

* Corresponding author at: Mark and Mary Stevens Neuroimaging and Informatics Institute, Keck School of Medicine of USC University of Southern California, 2025 Zonal Ave, Los Angeles, CA 90033, USA. Tel.: 323-442-7246; fax: 323-442-0137.
E-mail address: judypa@usc.edu (J. Pa).

https://doi.org/10.1016/j.neurobiolaging.2019.10.013

Notably, tumor necrosis factor-alpha (TNF-α) has been shown to be markedly elevated in patients with AD (Alsadany et al., 2013; Heneka and O'Banion, 2007; Liu et al., 2014), suggesting a chronic neuroinflammatory state that intensifies the secretion of associated cytokines and the duration of the immune response, which together may impact neuronal health. In fact, TNF-α, a member of the cytokine family, can directly impair neuronal function and suppress hippocampal long-term potentiation (LTP), a mechanism essential for memory storage and consolidation (Cunningham et al., 1996; Tancredi et al., 1992). For instance, young *APP*V717I transgenic mice show significantly decreased hippocampal LTP preceding amyloid plaque deposition (Heneka et al., 2005).

In human studies, elevated glial activation is associated with increased inflammatory cytokine activity including TNF-α in patients with mild to moderate dementia compared with healthy individuals (Cagnin et al., 2001; Paganelli et al., 2002; Tarkowski et al., 2003). Furthermore, in a neuropsychiatric population, elevated inflammation, as measured by other cytokines such as TNF-α and C-reactive protein (CRP) in plasma, has been associated with decreased cortical-striatal connectivity among those diagnosed as clinically depressed compared with normal adults (Felger et al., 2016). These studies suggest that cytokines such as TNF-α may directly impair neuronal function, either by measurement of LTP suppression or decreased functional connectivity (FC) and that early focal inflammatory events may contribute to neuronal dysfunction well before cell death. Activated glial cells are believed to modulate synaptic transmission (Bacci et al., 1999; Eroglu and Barres, 2010), and conversely, synaptic activity can induce activation of neuroimmune cells, resulting in neurogenic neuroinflammation (Tian et al., 2012). Collectively, these studies demonstrate a relationship between neuroinflammation and neural function, with chronic neuroinflammation leading to the loss of synapse associated proteins, thereby causing neuronal damage (Ma et al., 2014).

Although this evidence implicates a role of neuroinflammation in AD pathogenesis, little is known about the effect of TNF-α on brain FC. Large-scale changes in global brain function are known to be associated with early changes in the AD cascade using resting-state functional magnetic resonance imaging (rsfMRI) and brain network connectomics (Damoiseaux et al., 2012; Supekar et al., 2008). AD pathophysiology has long been associated with impaired synchrony among regions important for cognition. Recently, studies using rsfMRI in a brain connectomic framework have shown aberrant FC in the earliest stages of AD, concluding that abnormal FC may be one of the earliest indicators of neurodegeneration (Contreras et al., 2017, 2019). The aim of the present study was to first investigate a relationship between cerebrospinal fluid (CSF) inflammatory marker TNF-α and rsfMRI FC among our cohort, and, second, determine if *APOE*4 carrier status influences this relationship. Last, we hope to better characterize any differences based on *APOE*4 carrier status and clinical diagnosis using graph theory metrics.

2. Materials and methods

2.1. Participants

Our prospective study sample consisted of 64 older participants who were recruited through the Knight Alzheimer's Disease Research Center at Washington University at St. Louis. Study procedures were approved by the local Institutional Review Board and performed in accordance with the 1964 Declaration of Helsinki. Informed consent was obtained from all participants before study enrollment. Clinical diagnosis for each participant was based on standard criteria as incorporated in the Uniform Data Set (Morris et al., 2006). Participants were included based on availability of T1-weighted MPRAGE scan, rsfMRI scan, and CSF biomarker data. Specifically, there were 91 subjects with available CSF markers. Of those 91 subjects, 64 had available rsfMRI data. Therefore, we selected all of the 64 subjects with both CSF markers and rsfMRI to be included in this study. All biomarker assays and quantitative MRI scans were conducted by investigators blinded to the clinical status of the participant.

2.2. CSF biomarkers and genotyping

2.2.1. Inflammatory markers

Meso Scale Discovery (MSD) multiplex assay was used to determine CSF levels for TNF-α (Cat. No. K15049G, MSD, Rockville, MD, USA).

2.2.2. Amyloid-β peptide

Enzyme-linked immunosorbent assay was used to determine CSF Aβ42 in all participants (Cat. No. 81583, Innotest, Belgium).

2.2.3. Tau

MSD assay was used to determine CSF levels of total tau on all participants (Cat. No. K151LAE, MSD, Rockville, MD, USA), and enzyme-linked immunosorbent assay was used to determine phosphorylated tau (pT181) (Cat. No. 81581, Innotest, Belgium).

2.2.4. APOE genotyping

APOE genotyping was performed (as outlined in Nation et al. [2019]). Participants with at least one copy of the E4 gene were considered *APOE*4 carriers. There were no E2 homozygous or heterozygous carriers.

2.3. MRI data acquisition, processing, and analyses

2.3.1. Brain imaging acquisition

All images were obtained on a Siemens TrioTim 3T scanner using a 20-channel head coil. Anatomical T1-weighted 3D gradient echo pulse sequence scans were acquired with the following parameters: flip angle = 8°, TR/TE = 2400/3.16 ms, FOV 256 × 256 mm, voxel size was 1.1 × 1.1 × 1.2 mm^3 isotropic, length of scan = 7.04 minutes. rsfMRI scans were acquired eyes closed with the following parameters: flip angle 90°, TR/TE = 2200/27 ms, FOV 384 × 384 mm, voxel size: 4 mm^3 isotropic, scan time = 6.01 minutes.

2.3.2. Preprocessing and correlation analysis

rsfMRI images were preprocessed using the CONN-toolbox v18a ((Whitfield-Gabrieli and Nieto-Castanon, 2012): http://www.nitrc.org/projects/conn) in SPM12 for data analysis. The default preprocessing pipeline was utilized in which case, all functional images were realigned (motion corrected), centered, slice time–corrected, corrected for motion artifacts using the artifact detection tools, and coregistered to their corresponding structural images. Images were identified as outliers if the head movement (in direction x, y, z) was more than 5 standard deviations from the mean intensity of the entire run, or a 97th percentile threshold. All structural images were then centered and segmented into cerebrospinal fluid, gray and white matter, and spatially normalized to the Montreal Neurological Institute template. Functional images were then normalized to Montreal Neurological Institute space using the deformation field from the corresponding structural images and spatially smoothed to allow for better registration and reduction of noise using a 6 mm FWHM Gaussian kernel.

After preprocessing, the CompCor strategy (Behzadi et al., 2007) was implemented to account for white matter and CSF noise using principal component analysis. The analyses did not include global signal regression to avoid potential false anticorrelations (Murphy et al., 2009). Motion parameters, cerebrospinal fluid, and white

matter were included in the model and considered as variables of no interest. The mean BOLD signal time course was then extracted from every ROI and band pass filtered (0.009–0.09 Hz). To define our ROIs, we used the default-atlas implemented in the CONN toolbox (v18a) that uses a combination of the Harvard-Oxford atlas and the AAL atlas as well as a few commonly used ROIs from well-known networks and areas based of the work of Yeo et al (Yeo et al., 2011) and excluded cerebellar and primary sensory areas. Pearson's correlation coefficients were calculated for all pairwise comparisons between ROIs (see supplemental material, Appendix for complete list of ROIs used).

2.3.3. TNF-α-specific functional connectivity analysis and selection of seed region

To explore all possible associations between TNF-α and ROI to ROI functional connections, linear regression was used to compute the correlation between all pairwise ROIs FC strength and TNF-α. This allowed us to look at the matrix of effects between using all ROIs as potential "seeds" and all selected target ROIs while also correcting for multiple comparisons, using connection-level threshold (e.g., analysis-level FDR $p < 0.05$). Based on this analysis, the seed region was defined as the node with the strongest link between all ROIs and TNF-α, revealing the nucleus accumbens (NAcc). Other regions implicated in AD, such as the hippocampus and parahippocampus, were not found to be associated with TNF-α at FDR-corrected p-value < 0.05. In our analysis, we investigated regions functionally connected to either the L or R NAcc as seed region as well as investigating regions functionally connected to both L and R regions, which revealed similar results. Because there was no prior evidence to suggest left or right NAcc differed in their functional or anatomical role we chose to report on regions functionally connected to either the L or R NAcc as seed region. Age, sex, education, and diagnosis were included as model covariates, and all analyses were FDR-corrected ($p < 0.05$) for multiple comparisons. Moderation analysis was carried out using the PROCESS macro (Hayes, 2017) version 3.1 in SPSS version 25 to assess if the association between TNF-α and FC was moderated by *APOE*4 status.

2.3.4. Graph-based network analysis

Graph theory metrics including average path length, clustering coefficient, local efficiency and global efficiency were calculated using CONN toolbox to characterize the dynamics of FC within our cohort. These measures were calculated at the node level for our seed regions (NAcc left and right) as well as at the whole-brain network level using all ROIs listed in supplemental table 1. A graph adjacency matrix A (i, j) was computed by thresholding an ROI-to-ROI correlation matrix r (i, j) for each subject. To obtain a whole-brain network value for each metric for each subject, we averaged metric ROI values across the brain for each subject. Average path length was defined as the average of the shortest paths between each ROI and all other ROIs in the graph. Clustering coefficient, a measure of the degree to which nodes in a graph tend to cluster together, was calculated as the fraction of edges among all possible edges in the local neighboring subgraph for our seed ROI. Local efficiency represents a measure of local integration, characterizing the degree of interconnectedness of a node. Global efficiency, a measurement of node centrality within a network characterizing the global connectedness, was defined as the average of inverse distances between each ROI and all other ROIs in the graph. A detailed description of equations for graph theory metrics can be found at www.nitrc.org/projects/conn.

Partial correlation analysis was used to assess the relationship at the node level between graph theory metrics and TNF-α levels in *APOE*4 carriers and noncarriers and between diagnoses. One-way ANOVA was used to compare all metrics at the whole-brain network level between both *APOE*4 carriers and noncarriers as well as between diagnoses.

Last, the variance, skewness, and kurtosis were calculated to help characterize the group differences between AD and cognitively normal (CN) participants for the aforementioned graph theory metrics. The variance is the expectation of the squared deviation of the observation from the sample mean and therefore is concerned with the "spread" of the sample. Skewness is concerned with symmetry of the sample. A skewness of 0 means complete symmetry, a negative skew indicates a left tail, and a positive skew indicates a longer right tail. Kurtosis was used to measure the sharpness of the sample peak with higher values indicating a more well-defined mean and more observations around the tail(s). Smaller values indicate flatter distributions.

3. Results

3.1. Study participants

64 participants (30 CN, 34 mild AD) were included in this study. Of the total sample, 59% were men and 55% were *APOE*4 carriers. Participants were well educated with an average of 15.19 years of education. *APOE*4 carriers had significantly lower Aβ42 levels than noncarriers ($p < 0.05$), and a nonsignificant trend level difference in TNF-α ($p = 0.08$). There were no other significant differences between *APOE*4 carriers and noncarriers as indicated in Table 1.

3.2. TNF-α level is negatively correlated with resting-state functional connectivity

Linear regression was used to assess the association between higher TNF-α levels and lower FC strength among seed regions and all pairwise ROIs in all subjects (Fig. 1). To further explore the nature of this relationship, FDR-corrected p-values were plotted on matrices, split by *APOE*4 carrier status, revealing a possible E4 effect on the negative correlation between TNF-α and FC (Fig. 2). Age, sex, education, and diagnosis were included as covariates. The NAcc was identified as the key hub region, defined as the node with the strongest link between all ROIs and TNF-α, as seen in Fig. 1. Specifically, the connectivity between bilateral NAcc and the other 31 individual cortical regions was the best predictor of TNF-α levels across participants. Highly connected regions to NAcc included bilateral posterior middle temporal gyrus (MTG), anterior and posterior superior temporal gyrus, superior temporal gyrus, and temporal pole.

3.3. Moderation effect of APOE4 between TNF-α and FC

Connectivity between NAcc and posterior and anterior MTG had the strongest relationship with TNF-α ($p < 0.001$). *APOE*4 was a significant moderator of the relationship between lower FC and higher TNF-α levels. Fig. 2 helps visualize the moderating effect that *APOE*4 carriers has as seen by the FDR-corrected p-values along the NAcc column. Specifically, the presence of *APOE*4 allele moderated the relationship between TNF-α levels and FC in NAcc and posterior MTG (*APOE*4 carriers: TNF-α $\beta = -1.94$, $t(51) = -4.88$, $p = 0.00001$) and NAcc and anterior MTG (*APOE*4 carriers, TNF-α $\beta = -1.96$, $t(51) = -4.12$, $p = 0.0001$) (Fig. 3).

3.4. Graph theory metrics at the ROI level show differences between APOE4 carriers and noncarriers

Graph theory metrics for clustering coefficient, average path length, global efficiency, and local efficiency were calculated with the left and right NAcc to characterize the broader ROI connectivity

Table 1
Demographics for the study participants

Demographics	ALL-median (IQR)	*APOE*4 carriers (n = 34)		*APOE*4 noncarriers (n = 29)	
		AD	CN	AD	CN
Age (y)[b]	70.57 (12.93)	75.23 (7.97)	68.05 (16.59)	76.27 (11.50)	64.88 (18.08)
Sex (m/f)[a,b]	37/26	11/7	9/7	10/5	7/7
Education (y)	16 (5.5)	16 (5)	14 (2.5)	14 (5.25)	16 (2)
Diagnosis (AD/control)[a]	33/30	18	16	15	14
MMSE[b]	28 (5)	25.5 (4.5)	29 (2)	27 (7.5)	30 (1)
CDR score (0/0.5/1)[a]	30/25/8	1/13/4	15/1/0	0/11/4	14/0/0
Aβ-42 pg/mL[a,c,e]	529.667 (312.94)	319.45 (235.74)	581.07 (278.07)	505.19 (265.59)	643.08 (139.18)
T-Tau pg/mL[a,b,d]	361.9 (412.51)	553.18 (373.03)	309.51 (292.43)	468.25 (349.98)	202.99 (91.26)
P-Tau pg/mL	61.892 (43.87)	78.18 (69.38)	60.45 (34.68)	72.56 (46.29)	49.13 (24.74)
TNF-α pg/mL[e]	0.0939 (0.0809)	0.107 (0.081)	0.11 (0.114)	0.09 (0.0518)	0.0806 (0.0275)

Significance was tested using Mann-Whitney test.
Key: Aβ, amyloid-β; AD, Alzheimer's disease; *APOE*4, apolipoprotein E-ε4; CN, cognitively normal; TNF-α, tumor necrosis factor-alpha.
[a] indicates significant difference between *APOE4* carrier groups.
[b] indicates significant difference between AD/CN groups.
[c] indicates significant differences between *APOE4* carrier versus noncarrier subgroups of AD group.
[d] indicates significant differences between *APOE4* carrier versus non-carrier subgroups of CN group.
[e] indicates significant difference between CN in *APOE4* carrier group and AD in *APOE*4 noncarrier group. *APOE4* + participants carried a genotype of *APOE*3/4. *APOE*4- participants carried a genotype of *APOE*3/3.

patterns. Local efficiency and the clustering coefficient for the right NAcc were negatively correlated with TNF-α levels only in *APOE*4 carriers ($R^2 = 0.14$, β-coefficient $= -1.30$, $p = 0.04$; $R^2 = 0.15$, β-coefficient $= -1.21$, $p = 0.03$) (Fig. 4). Global efficiency and average path length were not correlated with TNF-α levels both when stratifying by *APOE*4 status.

3.5. Graph theory metrics at the whole-brain network level show differences based on clinical diagnosis

Clustering coefficient, average path length, global efficiency, and local efficiency were calculated on a whole-brain network level for each participant. A significant difference was found

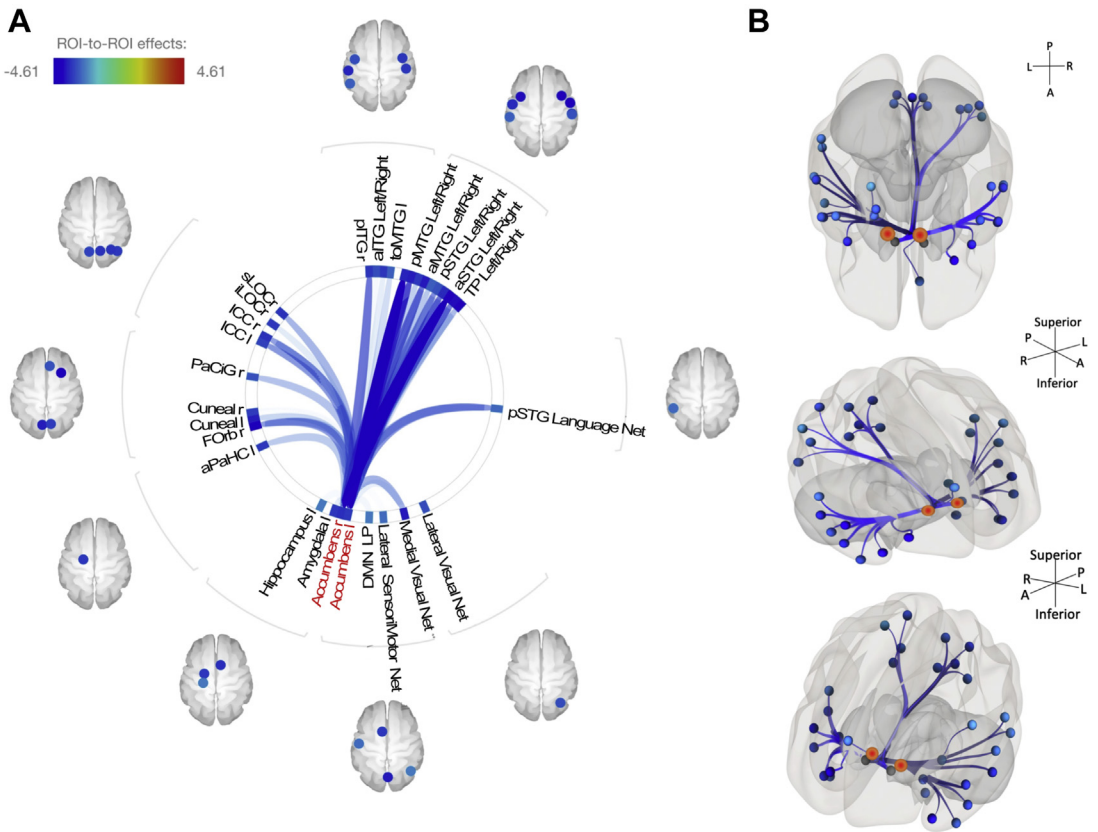

Fig. 1. Association between TNF-α and FC. Higher TNF-α levels were correlated with lower FC between NAcc (important for decision-making and inhibitory control) and regions involved in memory, visual processing, and language. (A) Connectogram with blue lines representing significant negative correlations between seed and targets after FDR correction. Opacity and width of line are proportional to FDR-corrected *p*-value. (B) Results are visualized anatomically on a brain. Red spheres indicate the NAcc as seed region and blue regions indicate significant ROIs (saturation of blue spheres proportional to *p*-value). Abbreviations: TNF-α, tumor necrosis factor-alpha; FC, functional connectivity; NAcc, nucleus accumbens.

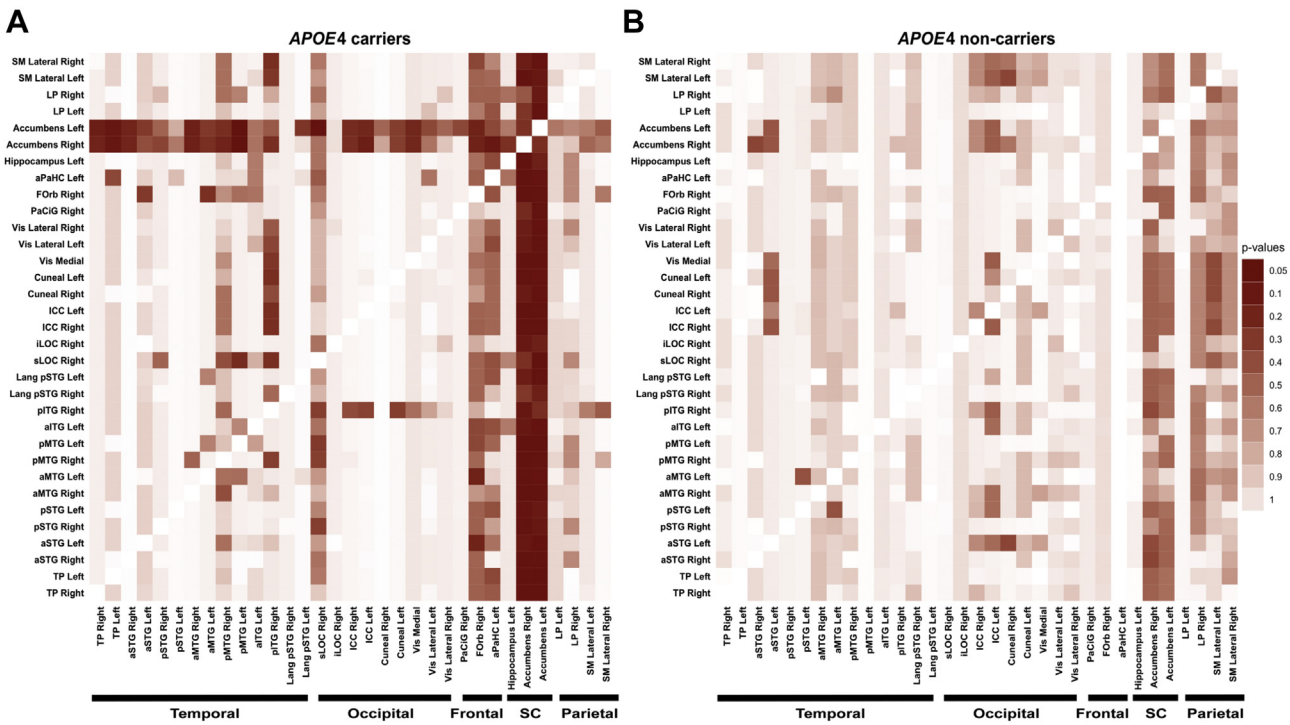

Fig. 2. Two-sided p-value matrices separated by APOE4 carrier status. Matrices, split by *APOE4* carrier status, show FDR-corrected *p*-values of linear regression model to show the relationship between TNF-α levels and FC values of ROIs. Connectivity between left and right NAcc and 31 individual cortical regions was significantly associated with TNF-α levels in *APOE4* carriers (A) relative to noncarriers (B) as visualized by the darker red color. Age, sex, education, and diagnosis were included as covariates. Columns represent seed regions; rows represent projection regions. Abbreviations: APOE4, apolipoprotein E-ε4; TNF-α, tumor necrosis factor-alpha; FC, functional connectivity; NAcc, nucleus accumbens.

between CN and AD participants among all graph theory metrics measuring whole-brain network characteristics (Table 2). Specifically, global efficiency was higher, whereas local efficiency, clustering coefficient, and average path length of the whole-brain network among AD individuals was lower compared with CN participants. In addition, for each metric, whole-brain network visualizations were plotted allowing for further observations regarding spatial change in network organization as well as plotting the distribution of values per metric by diagnosis to better quantify and characterize the change in network organization (Fig. 5). Variance was calculated to examine the spread of our sample, skewness to determine the symmetry of the sample/distribution, and kurtosis to measure the sharpness of the peak of our distribution (Table 2).

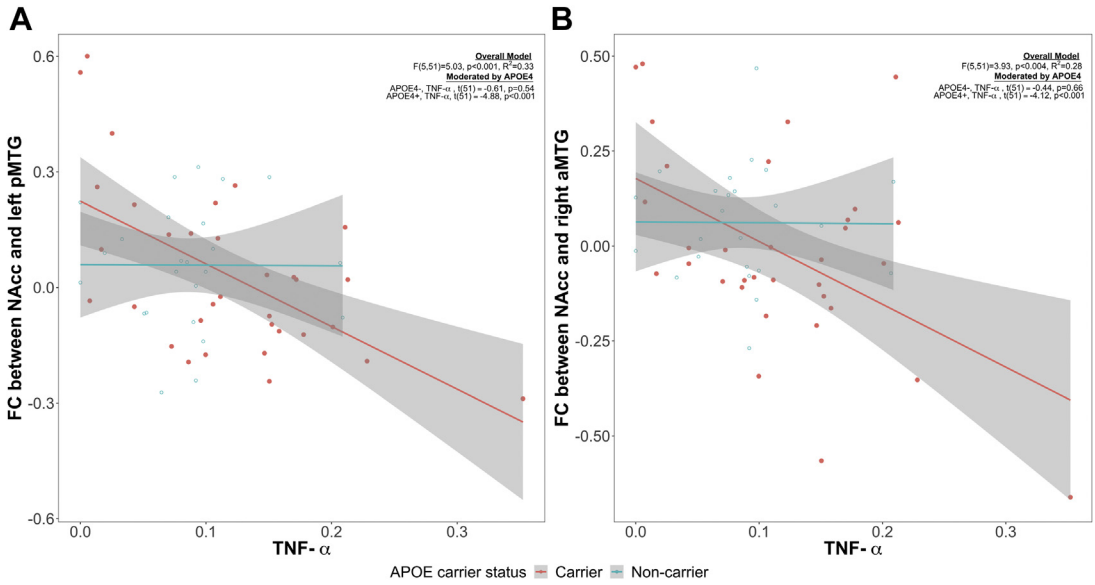

Fig. 3. Moderation analysis. *APOE4* carrier status moderates the relationship between TNF-α and functional connectivity of the NAcc to (A) left posterior MTG (pMTG) and to (B) anterior MTG (aMTG). APOE4 carriers had a stronger negative association between TNF-α and FC. Full model estimates are shown from the moderation analysis. Abbreviations: APOE4, apolipoprotein E-ε4; TNF-α, tumor necrosis factor-alpha; NAcc, nucleus accumbens.

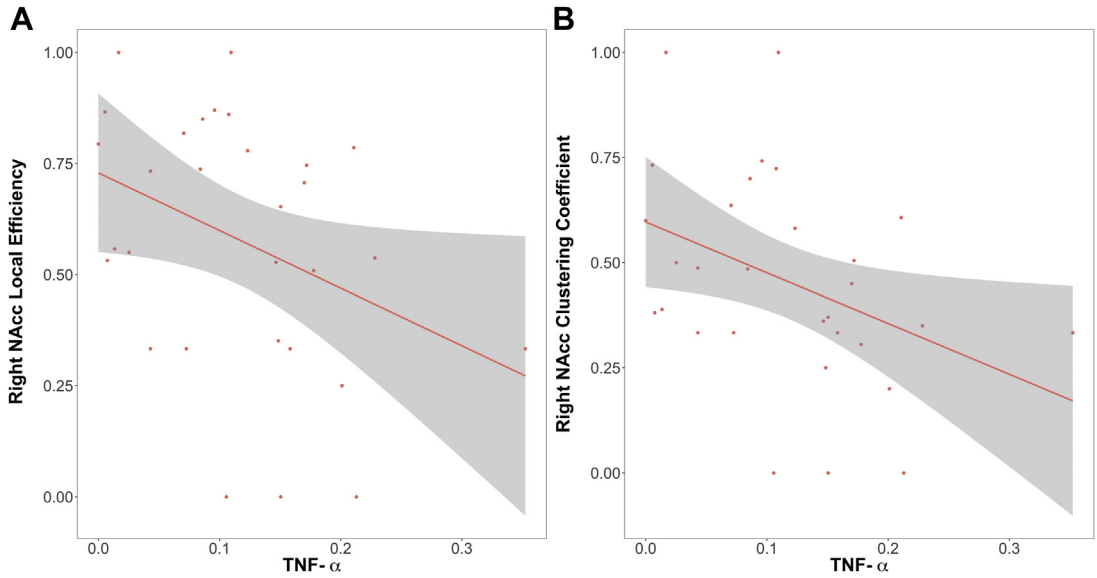

Fig. 4. Connectivity characteristics of NAcc node correlated with TNF-α only in APOE4 carriers. (A) Local efficiency and (B) clustering coefficient in the right NAcc were negatively correlated with TNF-α levels. Specifically, the right NAcc showed less integration with its neighboring ROIs and less clustering when TNF-α levels were high. Global efficiency and average path were not correlated with TNF-α. Abbreviations: APOE4, apolipoprotein E-ε4; TNF-α, tumor necrosis factor-alpha; NAcc, nucleus accumbens.

Within the AD group, overall variance was smaller indicating a loss of network organization as you reduce the inherent hierarchy of nodes (i.e., those acting as hub regions) that is normally present in a healthy brain and consisted of flatter distributions as indicated by a smaller kurtosis value (except in the case of global efficiency). Skewness tended to be more positive in the CN sample, signifying a greater network organizational structure. The difference in path lengths between AD and CN was the most visible (Fig. 5D). The CN group had lengthier paths (>2.72) and fewer shorter paths (<2.23) compared with the AD group. These shorter path lengths among the AD indicate a less integrated and more modular network pointing to a loss of organization within the AD participants' network.

Overall, local efficiency and clustering coefficient is disrupted in *APOE4* carriers relative to noncarriers at the ROI level, whereas all metrics at the global network level were disrupted in AD relative to CN.

4. Discussion

Our study sought to investigate the relationship between TNF-α, an inflammatory CSF cytokine relevant to AD, and rsfMRI FC. In doing so, we identified a functional connectivity network negatively affected by higher TNF-α levels especially among brain regions known to be important in decision-making and inhibitory control, but with implications for memory, language, and visual processing. On further analysis, this relationship with TNF-α was moderated by *APOE4* carrier status. Together, these findings support a heightened proinflammatory environment in *APOE4* carriers that impacts functional connectivity of cognitively meaningful networks that include brain regions NAcc and MTG.

Table 2
Connectivity characteristics between CN and AD participants

Measure	Group	Mean	Variance	Skewness	Kurtosis
Global efficiency	CN	**0.5009**	0.0022	−0.698	3.0281
	AD	**0.5125**	0.0017	−0.9601	4.0758
Local efficiency	CN	**0.7139**	**0.0033**	−0.3135	3.1841
	AD	**0.7**	**0.0023**	−0.2049	2.9144
Clustering coefficient	CN	**0.5214**	**0.0038**	0.7414	3.1858
	AD	**0.4937**	**0.0025**	0.4945	2.7032
Average path length	CN	**2.2716**	**0.0303**	0.8843	3.2139
	AD	**2.2031**	**0.0195**	0.7247	3.0054

Bold indicates significance ($p < 0.05$). There was a significant difference in all graph theory measures between AD and CN. There was no difference between *APOE4* carriers and noncarriers. We averaged metric ROI values across the brain for each subject to obtain a mean value per diagnosis. Additionally, we used variance, skewness and kurtosis to better characterize the difference in distributions between AD and CN for our respective graph theory metrics.
Key: AD, Alzheimer's disease; APOE4, apolipoprotein E-ε4; CN, cognitively normal.

The NAcc is central in the functional dopaminergic circuit involving the hippocampus and midbrain and plays a pivotal role in the formation of spatial memory, formation of novelty and persistent memory traces, as well as promoting reward directed behavior (Lisman and Grace, 2005; Roy et al., 2016; Russo and Nestler, 2013). Damage in these areas is presumably the principal cause for the onset of memory loss and both cognitive and noncognitive hallmarks of clinical AD (Squire et al., 2004; Wang and Morris, 2010). In fact, one study implicated that the circuit involving the hippocampus, midbrain and NAcc was severely impaired in an AD mouse model. This impairment resulted from a degeneration of dopaminergic neurons which is essential for correct functioning of the excitatory synaptic transmission between the NAcc and other regions (Cordella et al., 2018). In further support of the importance of the NAcc, another study found that atrophy in the NAcc (via reduced volume) correlated with clinical scores such as the MMSE and MOCA (Nie et al., 2017). Although the studies aforementioned show an important role of the NAcc in AD, our observations showing the relevance of NAcc FC in the context of neuroinflammation add new insight to its role in AD.

MTG has been implicated across many studies to serve a dynamic role in cognition, including semantic memory processing and language (Cabeza and Nyberg, 2000), observation of motion (Rizzolatti et al., 1996), deductive reasoning (Goel et al., 1998), dynamic facial expressions (Sato et al., 2012), and multimodal and higher sensory processing (Mesulam, 1998). Indeed, it has been proposed that MTG facilitates integration of information between ventral portions of inferior frontal gyrus and regions in the default mode network and executive network (Davey et al., 2016). Therefore, the MTG is spatially well positioned to serve as a hub

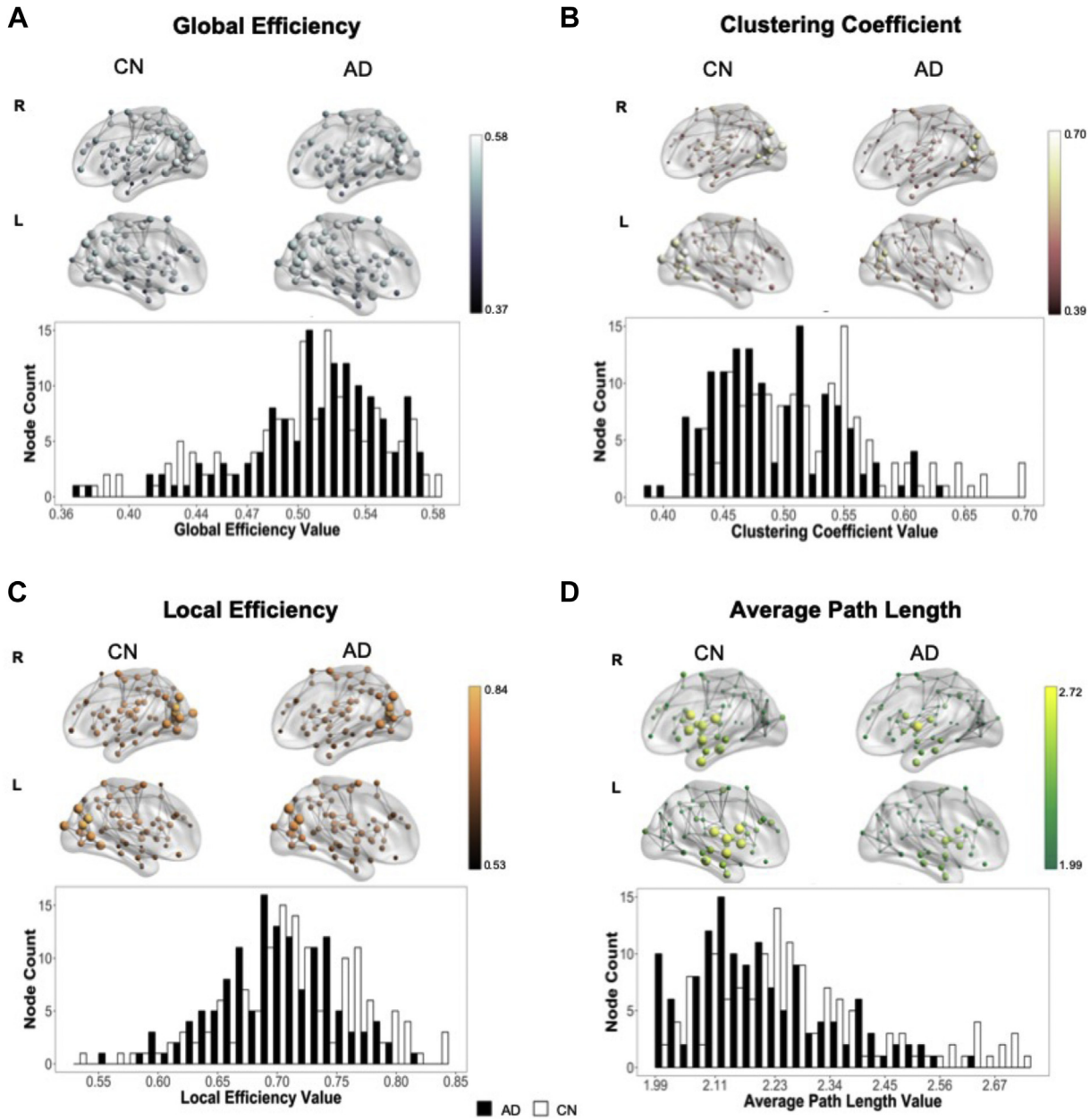

Fig. 5. Whole-brain network visualizations and distributions for each metric. Each graph theory metric is represented as a whole brain network between AD participants and CN participants. ROIs represent spherical nodes where size and color saturation indicate the numerical value of the metric (i.e., lighter color and larger node represent a larger graph theory metric). (A) Global efficiency values in R and L hemispheres between CN and AD participants. Histogram displays the distribution of the metric by diagnosis. The y-axis indicates how many nodes fall within a certain metric value. Here we see the difference in distributions between CN and AD. (B) Clustering coefficient, (C) local efficiency, and (D) average path. Within the AD group overall variance was smaller indicating a smaller spread of values and consisted of flatter distributions as indicated by a smaller kurtosis value (except in the case of global efficiency). Skewness tended to be greater in the CN sample, indicating a greater network organizational structure (with more high and low values, indicating the importance of certain nodes as compared with others). CN group had lengthier paths and fewer shorter paths compared with the AD group indicating a less integrated and more modular network for AD group. These differences in distribution indicate a loss of organization within the AD participants' network as graph theory metrics show less variance and narrower distribution reflecting a loss of high and low frequencies. Abbreviations: AD, Alzheimer's disease; CN, cognitively normal.

for the default mode network, language, and executive function networks. In support of this, a separate study demonstrated the left MTG as a hub using the participation coefficient (a measure of the distribution of a node's edges among the communities of a network and used to determine a node's "hubness" (Guimera and Nunes Amaral, 2005)). This study reported that left MTG mediates crosstalk between different functional modules in resting-state networks of those with social anxiety disorder (Yun et al., 2017). Furthermore, it was presumed that poorer cognitive functioning and presence of clinical symptoms (Kambeitz et al., 2016; van den Heuvel and Sporns, 2013; Warren et al., 2014) can result from lesions within important hub regions such as left MTG (Pannekoek et al., 2013; Qiu et al., 2014, 2015; Shang et al., 2014). Our results, showing strong reduced functional connectivity between and among these 2 important regions lend support to the more "integrated view" that acknowledges the synergy between different brain regions, shifting focus from a "neuron-centric" view which is restricted to local cell dysfunctions (Canter et al., 2016; Palop and Mucke, 2010).

We also examined the functional characteristics of our seed region to the entire network using all brain ROIs (Appendix). Because the NAcc receives information from a variety of systems that

promote distinct patterns of behavior, this region may play a more prominent role in other areas besides reward behavior. Therefore, we used graph theory metrics computing local, clustering, and global efficiency, as well as average path length for the left and right NAcc and overall brain network. We found that the right NAcc showed reduced local efficiency and clustering in *APOE*4 carriers with higher inflammation as measured by TNF-α. This suggests that the right NAcc showed less integration with its neighboring ROIs and less clustering when TNF-α levels were high. Global efficiency and average path length for NAcc were not correlated with TNF-α. The NAcc serves as a critical node within the brain's reward circuitry; yet, a more integrated role for this seed region proposed by Mogenson (Mogenson et al., 1993) suggests that the NAcc serves as a limbic-motor interface. Thus, the NAcc may be important for critical high-level tasks, including the selection of actions that help facilitate efficient goal-directed behavior (Floresco, 2015). These goals are set by frontal and temporal lobe regions with which the NAcc interfaces (Floresco et al., 1997; Floresco and Phillips, 1999; Ito et al., 2008; Mannella et al., 2013). Our results contribute to a growing body of literature that has reported differences between *APOE*4 carriers and noncarriers using graph theoretical measures at the ROI level (Filippini et al., 2009; Goryawala et al., 2014; Wink et al., 2018), and importantly highlight the relationship between inflammation, functional connectivity, and *APOE*4.

When we compared these graph theory metrics across the whole brain between clinical diagnoses (CN vs. AD), we found significant differences in all measurements, suggesting whole-brain network breakdown in those with clinical AD relative to CN participants. Important to note, the topological organization of a network is directly related to its local and global efficiency (Bullmore and Sporns, 2009; Rubinov and Sporns, 2010), as both are used to determine the brain network's capability of integrating information effectively. For instance, local efficiency provides an indication of how effectively information is integrated between immediate neighbors of a given node, whereas global efficiency provides an indication of how effectively information is integrated across the entire network. We found that while the functional network of participants with AD had a mean global efficiency value that was higher than our CN group among all ROIs, the number of ROIs with a high global efficiency value was less than that of the CN participants. This would indicate that there are fewer ROIs acting as central hub regions in the AD group (Buckner et al., 2009; He et al., 2008; Sporns et al., 2007). Participants with AD also had a greater number of ROIs with low local efficiency values as well as an overall lower local efficiency mean. This difference between global and local efficiency values between AD and CN groups indicates network organizational changes that may result in inadequate or inefficient transfer of information between ROIs, which is consistent with "small-world" organization that reflects the optimal balance between local processing and global integration in the human brain (Bassett and Bullmore, 2016).

Last, taking into consideration both clustering coefficiency and path length among ROIs, the network of participants with AD was less integrated and contained a more modular network resulting in reduced path lengths and lower clustering coefficiency values. Previous research has shown both resting-state network and modularity network differences between CN and AD groups and at various stages along the disease (Contreras et al., 2019; Sanz-Arigita et al., 2010; Supekar et al., 2008; Tijms et al., 2013; Wang et al., 2010, 2013). These results, taken together, may indicate a possible staging of early network breakdown at the local network level that is related to inflammation and that whole brain network breakdown follows along the spectrum of clinical disease.

Consistent with our findings, other studies have demonstrated higher inflammation and decreased functional connectivity in other patient populations. For instance, patients with major depressive disorder had reliably elevated cytokine levels, including CRP, interleukins 6, 1β, and 1 that were associated with decreased connectivity within striatal reward-related brain regions (i.e., putamen, caudate, and subdivisions on the striatum) (Felger et al., 2016). Similarly, nonhuman primate work has demonstrated that chronic administration of inflammatory cytokines decreased striatal dopamine release (Felger et al., 2007; Felger and Miller, 2012). Therefore, inflammation-related reductions in corticostriatal connectivity, may serve as a new pathophysiological pathway to explore in an effort to better understand how inflammation effects brain function and connectivity. Another study measured neuroinflammation via activated microglia using a PET radioactive tracer and found that AD-related neuroinflammation in white matter tissue of both mice and humans was increased compared with control mice (Raj et al., 2017). Because white matter tracts in the brain can be related to functional connectivity and speed of processing, compromised white matter integrity during aging can lead to symptomology such as compromised cognitive performance, as shown by de Lange et al (de Lange et al., 2016). They found differences in white matter integrity correlated to the participants' ability to adapt to demands of cognitive tasks and overall memory performance. In addition to the association between functional brain differences and inflammation, structural MRI studies have demonstrated a relationship between MRI markers of brain volume and CSF and plasma inflammation biomarkers in AD. A study with 42 participants with AD found a correlation between the CSF/serum IgG index and the indices of AD severity, including clinical dementia and medial temporal lobe atrophy (Matsumoto et al., 2008). Another study identified that 34 MRI volumetric brain regions (including the hippocampus, cingulate cortex, amygdala, and basal ganglia) combined with plasma cytokines and chemokines provided the best predictor of conversion from cognitive impairment to AD (Furney et al., 2011). Last, higher levels of systemic inflammation have been associated with reduced fractional anisotropy in white matter and lower cognition (Arfanakis et al., 2013). In a sample of nondemented older participants, systemic inflammation, assessed using a composite measure of inflammatory markers CRP and TNF-α, was found to negatively correlate with diffusion anisotropy in the corpus collosum and visual cognition suggesting inflammation is associated with lower microstructural integrity which leads to impaired higher-order visual cognition in aging adults. With evidence mounting on the effects of inflammation on large scale brain changes, it has become even more important to understand the role of inflammation on AD pathophysiology.

The amyloid cascade hypothesis states that deposition of Aβ is the causative agent of AD and that neurofibrillary tangles, inflammation, cell loss, vascular damage, and cognitive impairment are downstream effects of Aβ, with interactions between events (Hardy and Higgins, 1992; Selkoe, 1991). Yet, mounting evidence suggests that neuroinflammation may play a substantial role in Alzheimer's pathogenesis. While the interaction and temporal sequence of senile plaques, neurofibrillary tangles, and neuroinflammation remain inconclusive, animal models suggest neuroinflammation may contribute to the pathogenesis of plaques and tangles themselves (Zhang et al., 2013). This is underlined by findings that genes for immune receptors, such as *TREM2*, a microglial activation marker (Guerreiro et al., 2013) and *CD33*, also a microglial activation marker and thought to inhibit Aβ clearance (Bradshaw et al., 2013; Griciuc et al., 2013), are associated with AD. Analysis of clinical manifestations, which precede AD, such as mild cognitive impairment, further argues for substantial involvement of inflammation in the pathogenesis of AD.

4.1. Limitations and future directions

There are limitations to the present study. For instance, we were limited in that our *APOE*4 carriers were all heterogenous E3/4 carriers whereas our noncarriers were homozygous E3/3 carriers. Ideally, we would have liked to be able to parse out effects for those that were homozygous for E4 and any protective effects that E2 homozygous and heterozygous might have. It's also worth noting that we elected to use a specific brain parcellation scheme that also identifies ROIs belonging to particular resting state networks . It is possible that alternative anatomic and functional templates could return different results. Thus, future studies including multiple brain parcellation schemes and resting state network definitions would help determine the validity of our findings. We also acknowledge that better spatial resolution and improved acquisition parameters can greatly improve data quality as well as improve the stability and reproducibility of FC ROI-to-ROI results. Although this was not possible within this study, owing to the retrospective nature of the data, future studies will use superior methodology. In addition, we did not examine the role of other prominent inflammatory markers that may be modulating TNF-α such as IL-8, IL-6, as well as determining if blood-brain barrier (BBB) breakdown influences these relationships. We also recognize we were limited by the availability of clinical assessments as is the case with retrospective data. As much as 52% of clinical data were either missing, not collected, or incomplete. However, we are currently collecting additional data with similar variables (i.e., resting state fMRI data with advanced acquisition sequences, *APOE* genotype information availability, cognitive data) as well as CSF data that include a wide range of inflammatory markers and markers to measure BBB breakdown. These data will enable future studies to explore other markers and better establish a biological pathway for TNF-α (i.e., establish if vascular damage, via measuring BBB breakdown, leads to an increase in inflammatory markers).

In summary, we have provided evidence implicating neuroinflammation in *APOE*4 and AD, showing that higher CSF TNF-α levels are associated with lower FC between brain regions important in decision-making and inhibitory control in *APOE*4 carriers. Investigating inflammation and functional connectivity in older adults at risk for AD may help us better understand how the immune system contributes to the pathogenesis of AD.

Disclosure

The authors have no conflict of interest to disclose.

Acknowledgements

The authors thank the participants who generously donated their time and effort to make this research possible. In addition, the authors thank Dr. Daniel Albrecht for his intellectual input and support.

This work was supported by the National Institute on Aging grants P01AG03991, P50AG05681, P01AG026276 (JC Morris PI), P01AG052350 (B Zlokovic), and R01AG054617 (J Pa, PI).

Appendix A. Supplementary data

Supplementary data to this article can be found online at https://doi.org/10.1016/j.neurobiolaging.2019.10.013.

References

Akiyama, H., Arai, T., Kondo, H., Tanno, E., Haga, C., Ikeda, K., 2000. Cell mediators of inflammation in the Alzheimer disease brain. Alzheimer Dis. Assoc. Disord. 14 (Suppl.1), S47–S53.

Alsadany, M.A., Shehata, H.H., Mohamad, M.I., Mahfouz, R.G., 2013. Histone deacetylases enzyme, copper, and IL-8 levels in patients with Alzheimer's disease. Am. J. Alzheimers Dis. Other Demen. 28, 54–61.

Ardura-Fabregat, A., Boddeke, E., Boza-Serrano, A., Brioschi, S., Castro-Gomez, S., Ceyzeriat, K., Dansokho, C., Dierkes, T., Gelders, G., Heneka, M.T., Hoeijmakers, L., Hoffmann, A., Iaccarino, L., Jahnert, S., Kuhbandner, K., Landreth, G., Lonnemann, N., Loschmann, P.A., McManus, R.M., Paulus, A., Reemst, K., Sanchez-Caro, J.M., Tiberi, A., Van der Perren, A., Vautheny, A., Venegas, C., Webers, A., Weydt, P., Wijasa, T.S., Xiang, X., Yang, Y., 2017. Targeting neuroinflammation to treat Alzheimer's disease. CNS Drugs 31, 1057–1082.

Arfanakis, K., Fleischman, D.A., Grisot, G., Barth, C.M., Varentsova, A., Morris, M.C., Barnes, L.L., Bennett, D.A., 2013. Systemic inflammation in non-demented elderly human subjects: brain microstructure and cognition. PLoS One 8, e73107.

Bacci, A., Verderio, C., Pravettoni, E., Matteoli, M., 1999. The role of glial cells in synaptic function. Philos. Trans. R Soc. Lond. B Biol. Sci. 354, 403–409.

Bassett, D.S., Bullmore, E.T., 2016. Small-world brain networks revisited. Neuroscientist 23, 499–516.

Behzadi, Y., Restom, K., Liau, J., Liu, T.T., 2007. A component based noise correction method (CompCor) for BOLD and perfusion based fMRI. Neuroimage 37, 90–101.

Bradshaw, E.M., Chibnik, L.B., Keenan, B.T., Ottoboni, L., Raj, T., Tang, A., Rosenkrantz, L.L., Imboywa, S., Lee, M., Von Korff, A., Morris, M.C., Evans, D.A., Johnson, K., Sperling, R.A., Schneider, J.A., Bennett, D.A., De Jager, P.L., 2013. CD33 Alzheimer's disease locus: altered monocyte function and amyloid biology. Nat. Neurosci. 16, 848–850.

Breunig, J.J., Guillot-Sestier, M.V., Town, T., 2013. Brain injury, neuroinflammation and Alzheimer's disease. Front Aging Neurosci. 5, 26.

Bronzuoli, M.R., Iacomino, A., Steardo, L., Scuderi, C., 2016. Targeting neuroinflammation in Alzheimer's disease. J. Inflamm. Res. 9, 199–208.

Buckner, R.L., Sepulcre, J., Talukdar, T., Krienen, F.M., Liu, H., Hedden, T., Andrews-Hanna, J.R., Sperling, R.A., Johnson, K.A., 2009. Cortical hubs revealed by intrinsic functional connectivity: mapping, assessment of stability, and relation to Alzheimer's disease. J. Neurosci. 29, 1860–1873.

Bullmore, E., Sporns, O., 2009. Complex brain networks: graph theoretical analysis of structural and functional systems. Nat. Rev. Neurosci. 10, 186–198.

Cabeza, R., Nyberg, L., 2000. Imaging cognition II: an empirical review of 275 PET and fMRI studies. J. Cogn. Neurosci. 12, 1–47.

Cagnin, A., Brooks, D.J., Kennedy, A.M., Gunn, R.N., Myers, R., Turkheimer, F.E., Jones, T., Banati, R.B., 2001. In-vivo measurement of activated microglia in dementia. Lancet 358, 461–467.

Canter, R.G., Penney, J., Tsai, L.H., 2016. The road to restoring neural circuits for the treatment of Alzheimer's disease. Nature 539, 187.

Contreras, J.A., Avena-Koenigsberger, A., Risacher, S.L., West, J.D., Tallman, E., McDonald, B.C., Farlow, M.R., Apostolova, L.G., Goni, J., Dzemidzic, M., Wu, Y.C., Kessler, D., Jeub, L., Fortunato, S., Saykin, A.J., Sporns, O., 2019. Resting state network modularity along the prodromal late onset Alzheimer's disease continuum. Neuroimage Clin. 22, 101687.

Contreras, J.A., Goni, J., Risacher, S.L., Amico, E., Yoder, K., Dzemidzic, M., West, J.D., McDonald, B.C., Farlow, M.R., Sporns, O., Saykin, A.J., 2017. Cognitive complaints in older adults at risk for Alzheimer's disease are associated with altered resting-state networks. Alzheimers Dement. (Amst.) 6, 40–49.

Cordella, A., Krashia, P., Nobili, A., Pignataro, A., La Barbera, L., Viscomi, M.T., Valzania, A., Keller, F., Ammassari-Teule, M., Mercuri, N.B., Berretta, N., D'Amelio, M., 2018. Dopamine loss alters the hippocampus-nucleus accumbens synaptic transmission in the Tg2576 mouse model of Alzheimer's disease. Neurobiol. Dis. 116, 142–154.

Cunningham, A.J., Murray, C.A., O'Neill, L.A.J., Lynch, M.A., O'Connor, J.J., 1996. Interleukin-1β (IL-1β) and tumour necrosis factor (TNF) inhibit long-term potentiation in the rat dentate gyrus in vitro. Neurosci. Lett. 203, 17–20.

Damoiseaux, J.S., Prater, K.E., Miller, B.L., Greicius, M.D., 2012. Functional connectivity tracks clinical deterioration in Alzheimer's disease. Neurobiol. Aging 33, 828.e19–828.e30.

Davey, J., Thompson, H.E., Hallam, G., Karapanagiotidis, T., Murphy, C., De Caso, I., Krieger-Redwood, K., Bernhardt, B.C., Smallwood, J., Jefferies, E., 2016. Exploring the role of the posterior middle temporal gyrus in semantic cognition: integration of anterior temporal lobe with executive processes. Neuroimage 137, 165–177.

de Lange, A.G., Brathen, A.C., Grydeland, H., Sexton, C., Johansen-Berg, H., Andersson, J.L., Rohani, D.A., Nyberg, L., Fjell, A.M., Walhovd, K.B., 2016. White matter integrity as a marker for cognitive plasticity in aging. Neurobiol. Aging 47, 74–82.

den Hartigh, L.J., Altman, R., Hutchinson, R., Petrlova, J., Budamagunta, M.S., Tetali, S.D., Lagerstedt, J.O., Voss, J.C., Rutledge, J.C., 2012. Postprandial apoE isoform and conformational changes associated with VLDL lipolysis products modulate monocyte inflammation. PLoS One 7, e50513.

Dudal, S., Krzywkowski, P., Paquette, J., Morissette, C., Lacombe, D., Tremblay, P., Gervais, F., 2004. Inflammation occurs early during the Abeta deposition process in TgCRND8 mice. Neurobiol. Aging 25, 861–871.

Eroglu, C., Barres, B.A., 2010. Regulation of synaptic connectivity by glia. Nature 468, 223–231.
Felger, J.C., Alagbe, O., Hu, F., Mook, D., Freeman, A.A., Sanchez, M.M., Kalin, N.H., Ratti, E., Nemeroff, C.B., Miller, A.H., 2007. Effects of interferon-alpha on rhesus monkeys: a nonhuman primate model of cytokine-induced depression. Biol. Psychiatry 62, 1324–1333.
Felger, J.C., Li, Z., Haroon, E., Woolwine, B.J., Jung, M.Y., Hu, X., Miller, A.H., 2016. Inflammation is associated with decreased functional connectivity within corticostriatal reward circuitry in depression. Mol. Psychiatry 21, 1358–1365.
Felger, J.C., Miller, A.H., 2012. Cytokine effects on the basal ganglia and dopamine function: the subcortical source of inflammatory malaise. Front Neuroendocrinol 33, 315–327.
Filippini, N., Rao, A., Wetten, S., Gibson, R.A., Borrie, M., Guzman, D., Kertesz, A., Loy-English, I., Williams, J., Nichols, T., Whitcher, B., Matthews, P.M., 2009. Anatomically-distinct genetic associations of APOE epsilon4 allele load with regional cortical atrophy in Alzheimer's disease. Neuroimage 44, 724–728.
Floresco, S.B., 2015. The nucleus accumbens: an interface between cognition, emotion, and action. Annu. Rev. Psychol. 66, 25–52.
Floresco, S.B., Phillips, A.G., 1999. Dopamine and hippocampal input to the nucleus accumbens play an essential role in the search for food in an unpredictable environment. Psychobiology 27, 277–286.
Floresco, S.B., Seamans, J.K., Phillips, A.G., 1997. Selective roles for hippocampal, prefrontal cortical, and ventral striatal circuits in radial-arm maze tasks with or without a delay. J. Neurosci. 17, 1880–1890.
Furney, S.J., Kronenberg, D., Simmons, A., Guntert, A., Dobson, R.J., Proitsi, P., Wahlund, L.O., Kloszewska, I., Mecocci, P., Soininen, H., Tsolaki, M., Vellas, B., Spenger, C., Lovestone, S., 2011. Combinatorial markers of mild cognitive impairment conversion to Alzheimer's disease–cytokines and MRI measures together predict disease progression. J. Alzheimers Dis. 26 (Suppl.3), 395–405.
Goel, V., Gold, B., Kapur, S., Houle, S., 1998. Neuroanatomical correlates of human reasoning. Journal of Cognitive Neuroscience. J. Cogn. Neurosci. 10, 293–302.
Goryawala, M., Zhou, Q., Duara, R., Loewenstein, D., Cabrerizo, M., Barker, W., Adjouadi, M., 2014. Altered small-world anatomical networks in Apolipoprotein-E4 (ApoE4) carriers using MRI. Conf. Proc. IEEE Eng. Med. Biol. Soc. 2014, 2468–2471.
Griciuc, A., Serrano-Pozo, A., Parrado, A.R., Lesinski, A.N., Asselin, C.N., Mullin, K., Hooli, B., Choi, S.H., Hyman, B.T., Tanzi, R.E., 2013. Alzheimer's disease risk gene CD33 inhibits microglial uptake of amyloid beta. Neuron 78, 631–643.
Guerreiro, R., Wojtas, A., Bras, J., Carrasquillo, M., Rogaeva, E., Majounie, E., Cruchaga, C., Sassi, C., Kauwe, J.S., Younkin, S., Hazrati, L., Collinge, J., Pocock, J., Lashley, T., Williams, J., Lambert, J.C., Amouyel, P., Goate, A., Rademakers, R., Morgan, K., Powell, J., St George-Hyslop, P., Singleton, A., Hardy, J., 2013. TREM2 variants in Alzheimer's disease. N. Engl. J. Med. 368, 117–127.
Guimera, R., Nunes Amaral, L.A., 2005. Functional cartography of complex metabolic networks. Nature 433, 895–900.
Guo, L., LaDu, M.J., Van Eldik, L.J., 2004. A dual role for apolipoprotein e in neuroinflammation: anti- and pro-inflammatory activity. J. Mol. Neurosci. 23, 205–212.
Hardy, J.A., Higgins, G.A., 1992. Alzheimer's disease: the amyloid cascade hypothesis. Science 256, 184–185.
Hayes, A.F., 2017. Methodology in the Social Sciences. Introduction to Mediation, Moderation, and Conditional Process Analysis: A Regression-Based Approach. Guilford Press, New York, NY, US.
He, Y., Chen, Z., Evans, A., 2008. Structural insights into aberrant topological patterns of large-scale cortical networks in Alzheimer's disease. J. Neurosci. 28, 4756–4766.
Heneka, M.T., Carson, M.J., El Khoury, J., Landreth, G.E., Brosseron, F., Feinstein, D.L., Jacobs, A.H., Wyss-Coray, T., Vitorica, J., Ransohoff, R.M., Herrup, K., Frautschy, S.A., Finsen, B., Brown, G.C., Verkhratsky, A., Yamanaka, K., Koistinaho, J., Latz, E., Halle, A., Petzold, G.C., Town, T., Morgan, D., Shinohara, M.L., Perry, V.H., Holmes, C., Bazan, N.G., Brooks, D.J., Hunot, S., Joseph, B., Deigendesch, N., Garaschuk, O., Boddeke, E., Dinarello, C.A., Breitner, J.C., Cole, G.M., Golenbock, D.T., Kummer, M.P., 2015. Neuroinflammation in Alzheimer's disease. Lancet Neurol. 14, 388–405.
Heneka, M.T., O'Banion, M.K., 2007. Inflammatory processes in Alzheimer's disease. J. Neuroimmunol. 184, 69–91.
Heneka, M.T., Sastre, M., Dumitrescu-Ozimek, L., Dewachter, I., Walter, J., Klockgether, T., Van Leuven, F., 2005. Focal glial activation coincides with increased BACE1 activation and precedes amyloid plaque deposition in APP [V717I] transgenic mice. J. Neuroinflammation 2, 22.
Ito, R., Robbins, T.W., Pennartz, C.M., Everitt, B.J., 2008. Functional interaction between the hippocampus and nucleus accumbens shell is necessary for the acquisition of appetitive spatial context conditioning. J. Neurosci. 28, 6950–6959.
Kambeitz, J., Kambeitz-Ilankovic, L., Cabral, C., Dwyer, D.B., Calhoun, V.D., van den Heuvel, M.P., Falkai, P., Koutsouleris, N., Malchow, B., 2016. Aberrant functional whole-brain network architecture in patients with Schizophrenia: a meta-analysis. Schizophr. Bull. 42 (Suppl.1), S13–S21.
Lisman, J.E., Grace, A.A., 2005. The hippocampal-VTA loop: controlling the entry of information into long-term memory. Neuron 46, 703–713.
Liu, S., Wang, X., Li, Y., Xu, L., Yu, X., Ge, L., Li, J., Zhu, Y., He, S., 2014. Necroptosis mediates TNF-induced toxicity of hippocampal neurons. Biomed. Res. Int. 2014, 290182.
Liu, Y., Xu, X., Dou, H., Hua, Y., Xu, J., Hui, X., 2015. Apolipoprotein E knockout induced inflammatory responses related to microglia in neonatal mice brain via astrocytes. Int. J. Clin. Exp. Med. 8, 737–743.
Ma, J., Choi, B.R., Chung, C., Min, S.S., Jeon, W.K., Han, J.S., 2014. Chronic brain inflammation causes a reduction in GluN2A and GluN2B subunits of NMDA receptors and an increase in the phosphorylation of mitogen-activated protein kinases in the hippocampus. Mol. Brain 7, 33.
Mannella, F., Gurney, K., Baldassarre, G., 2013. The nucleus accumbens as a nexus between values and goals in goal-directed behavior: a review and a new hypothesis. Front Behav. Neurosci. 7, 135.
Matsumoto, Y., Yanase, D., Noguchi-Shinohara, M., Ono, K., Yoshita, M., Yamada, M., 2008. Cerebrospinal fluid/serum IgG index is correlated with medial temporal lobe atrophy in Alzheimer's disease. Dement. Geriatr. Cogn. Disord. 25, 144–147.
Mesulam, M.M., 1998. From sensation to cognition. Brain 121 (Pt 6), 1013–1052.
Mogenson, G.J., Brudzynski, S.M., Wu, M., Yang, C.R., Yim, C.C.Y., 1993. From motivation to action: a review of dopaminergic regulation of limbic→nucleus accumbens→ventral pallidum→pedunculopontine nucleus circuitries involved in limbic motor integration. Limbic Mot. Circuits Neuropsychiatry 193–236.
Morris, J.C., Weintraub, S., Chui, H.C., Cummings, J., Decarli, C., Ferris, S., Foster, N.L., Galasko, D., Graff-Radford, N., Peskind, E.R., Beekly, D., Ramos, E.M., Kukull, W.A., 2006. The Uniform data set (UDS): clinical and cognitive variables and descriptive data from Alzheimer disease centers. Alzheimer Dis. Assoc. Disord. 20, 210–216.
Murphy, K., Birn, R.M., Handwerker, D.A., Jones, T.B., Bandettini, P.A., 2009. The impact of global signal regression on resting state correlations: are anti-correlated networks introduced? Neuroimage 44, 893–905.
Nation, D.A., Sweeney, M.D., Montagne, A., Sagare, A.P., D'Orazio, L.M., Pachicano, M., Sepehrband, F., Nelson, A.R., Buennagel, D.P., Harrington, M.G., Benzinger, T.L.S., Fagan, A.M., Ringman, J.M., Schneider, L.S., Morris, J.C., Chui, H.C., Law, M., Toga, A.W., Zlokovic, B.V., 2019. Blood-brain barrier breakdown is an early biomarker of human cognitive dysfunction. Nat. Med. 25, 270–276.
Nie, X., Sun, Y., Wan, S., Zhao, H., Liu, R., Li, X., Wu, S., Nedelska, Z., Hort, J., Qing, Z., Xu, Y., Zhang, B., 2017. Subregional structural alterations in Hippocampus and nucleus accumbens correlate with the clinical impairment in patients with Alzheimer's disease clinical spectrum: parallel combining volume and vertex-based approach. Front Neurol. 8, 399.
Paganelli, R., Di Iorio, A., Patricelli, L., Ripani, F., Sparvieri, E., Faricelli, R., Iarlori, C., Porreca, E., Di Gioacchino, M., Abate, G., 2002. Proinflammatory cytokines in sera of elderly patients with dementia: levels in vascular injury are higher than those of mild-moderate Alzheimer's disease patients. Exp. Gerontol. 37, 257–263.
Palop, J.J., Mucke, L., 2010. Amyloid-β–induced neuronal dysfunction in Alzheimer's disease: from synapses toward neural networks. Nat. Neurosci. 13, 812.
Pannekoek, J.N., Veer, I.M., van Tol, M.J., van der Werff, S.J., Demenescu, L.R., Aleman, A., Veltman, D.J., Zitman, F.G., Rombouts, S.A., van der Wee, N.J., 2013. Resting-state functional connectivity abnormalities in limbic and salience networks in social anxiety disorder without comorbidity. Eur. Neuropsychopharmacol. 23, 186–195.
Qiu, C., Feng, Y., Meng, Y., Liao, W., Huang, X., Lui, S., Zhu, C., Chen, H., Gong, Q., Zhang, W., 2015. Analysis of altered baseline brain activity in drug-naive adult patients with social anxiety disorder using resting-state functional MRI. Psychiatry Investig. 12, 372–380.
Qiu, C., Zhu, C., Zhang, J., Nie, X., Feng, Y., Meng, Y., Wu, R., Huang, X., Zhang, W., Gong, Q., 2014. Diffusion tensor imaging studies on Chinese patients with social anxiety disorder. Biomed. Res. Int. 2014, 860658.
Raj, D., Yin, Z., Breur, M., Doorduin, J., Holtman, I.R., Olah, M., Mantingh-Otter, I.J., Van Dam, D., De Deyn, P.P., den Dunnen, W., Eggen, B.J.L., Amor, S., Boddeke, E., 2017. Increased white matter inflammation in aging- and Alzheimer's disease brain. Front Mol. Neurosci. 10, 206.
Rizzolatti, G., Fadiga, L., Matelli, M., Bettinardi, V., Paulesu, E., Perani, D., Fazio, F., 1996. Localization of grasp representations in humans by PET: 1. Observation versus execution. Exp. Brain Res. 111, 246–252.
Rodriguez, G.A., Tai, L.M., LaDu, M.J., Rebeck, G.W., 2014. Human APOE4 increases microglia reactivity at Abeta plaques in a mouse model of Abeta deposition. J. Neuroinflammation 11, 111.
Roy, D.S., Arons, A., Mitchell, T.I., Pignatelli, M., Ryan, T.J., Tonegawa, S., 2016. Memory retrieval by activating engram cells in mouse models of early Alzheimer's disease. Nature 531, 508.
Rubinov, M., Sporns, O., 2010. Complex network measures of brain connectivity: uses and interpretations. Neuroimage 52, 1059–1069.
Russo, S.J., Nestler, E.J., 2013. The brain reward circuitry in mood disorders. Nat. Rev. Neurosci. 14, 609.
Sanz-Arigita, E.J., Schoonheim, M.M., Damoiseaux, J.S., Rombouts, S.A., Maris, E., Barkhof, F., Scheltens, P., Stam, C.J., 2010. Loss of 'small-world' networks in Alzheimer's disease: graph analysis of FMRI resting-state functional connectivity. PLoS One 5, e13788.
Sato, W., Toichi, M., Uono, S., Kochiyama, T., 2012. Impaired social brain network for processing dynamic facial expressions in autism spectrum disorders. BMC Neurosci. 13, 99.
Selkoe, D.J., 1991. The molecular pathology of Alzheimer's disease. Neuron 6, 487–498.
Shang, J., Fu, Y., Ren, Z., Zhang, T., Du, M., Gong, Q., Lui, S., Zhang, W., 2014. The common traits of the ACC and PFC in anxiety disorders in the DSM-5: meta-analysis of voxel-based morphometry studies. PLoS One 9, e93432.

Sporns, O., Honey, C.J., Kotter, R., 2007. Identification and classification of hubs in brain networks. PLoS One 2, e1049.
Squire, L.R., Stark, C.E.L., Clark, R.E., 2004. The medial temporal lobe. Annu. Rev. Neurosci. 27, 279–306.
Supekar, K., Menon, V., Rubin, D., Musen, M., Greicius, M.D., 2008. Network analysis of intrinsic functional brain connectivity in Alzheimer's disease. PLoS Comput. Biol. 4, e1000100.
Sweeney, M.D., Sagare, A.P., Zlokovic, B.V., 2015. Cerebrospinal fluid biomarkers of neurovascular dysfunction in mild dementia and Alzheimer's disease. J. Cereb. Blood Flow Metab. 35, 1055–1068.
Tan, J., Town, T., Mullan, M., 2002. CD40-CD40L interaction in Alzheimer's disease. Curr. Opin. Pharmacol. 2, 445–451.
Tancredi, V., D'Arcangelo, G., Grassi, F., Tarroni, P., Palmieri, G., Santoni, A., Eusebi, F., 1992. Tumor necrosis factor alters synaptic transmission in rat hippocampal slices. Neurosci. Lett. 146, 176–178.
Tarkowski, E., Liljeroth, A.M., Minthon, L., Tarkowski, A., Wallin, A., Blennow, K., 2003. Cerebral pattern of pro- and anti-inflammatory cytokines in dementias. Brain Res. Bull 61, 255–260.
Tian, L., Ma, L., Kaarela, T., Li, Z., 2012. Neuroimmune crosstalk in the central nervous system and its significance for neurological diseases. J. Neuroinflammation 9, 155.
Tijms, B.M., Wink, A.M., de Haan, W., van der Flier, W.M., Stam, C.J., Scheltens, P., Barkhof, F., 2013. Alzheimer's disease: connecting findings from graph theoretical studies of brain networks. Neurobiol. Aging 34, 2023–2036.
van den Heuvel, M.P., Sporns, O., 2013. Network hubs in the human brain. Trends Cogn. Sci. 17, 683–696.
Vitek, M.P., Brown, C.M., Colton, C.A., 2009. APOE genotype-specific differences in the innate immune response. Neurobiol. Aging 30, 1350–1360.
Wang, J., Zuo, X., Dai, Z., Xia, M., Zhao, Z., Zhao, X., Jia, J., Han, Y., He, Y., 2013. Disrupted functional brain connectome in individuals at risk for Alzheimer's disease. Biol. Psychiatry 73, 472–481.
Wang, J., Zuo, X., He, Y., 2010. Graph-based network analysis of resting-state functional MRI. Front Syst. Neurosci. 4, 16.
Wang, S.-H., Morris, R.G.M., 2010. Hippocampal-neocortical interactions in memory formation, consolidation, and reconsolidation. Annu. Rev. Psychol. 61, 49–79.
Warren, D.E., Power, J.D., Bruss, J., Denburg, N.L., Waldron, E.J., Sun, H., Petersen, S.E., Tranel, D., 2014. Network measures predict neuropsychological outcome after brain injury. Proc. Natl. Acad. Sci. U. S. A. 111, 14247–14252.
Whitfield-Gabrieli, S., Nieto-Castanon, A., 2012. Conn: a functional connectivity toolbox for correlated and anticorrelated brain networks. Brain Connect. 2, 125–141.
Wink, A.M., Tijms, B.M., Ten Kate, M., Raspor, E., de Munck, J.C., Altena, E., Ecay-Torres, M., Clerigue, M., Estanga, A., Garcia-Sebastian, M., Izagirre, A., Martinez-Lage Alvarez, P., Villanua, J., Barkhof, F., Sanz-Arigita, E., 2018. Functional brain network centrality is related to APOE genotype in cognitively normal elderly. Brain Behav. 8, e01080.
Yeo, B.T., Krienen, F.M., Sepulcre, J., Sabuncu, M.R., Lashkari, D., Hollinshead, M., Roffman, J.L., Smoller, J.W., Zollei, L., Polimeni, J.R., Fischl, B., Liu, H., Buckner, R.L., 2011. The organization of the human cerebral cortex estimated by intrinsic functional connectivity. J. Neurophysiol. 106, 1125–1165.
Yun, J.Y., Kim, J.C., Ku, J., Shin, J.E., Kim, J.J., Choi, S.H., 2017. The left middle temporal gyrus in the middle of an impaired social-affective communication network in social anxiety disorder. J. Affect. Disord. 214, 53–59.
Zhang, B., Gaiteri, C., Bodea, L.G., Wang, Z., McElwee, J., Podtelezhnikov, A.A., Zhang, C., Xie, T., Tran, L., Dobrin, R., Fluder, E., Clurman, B., Melquist, S., Narayanan, M., Suver, C., Shah, H., Mahajan, M., Gillis, T., Mysore, J., MacDonald, M.E., Lamb, J.R., Bennett, D.A., Molony, C., Stone, D.J., Gudnason, V., Myers, A.J., Schadt, E.E., Neumann, H., Zhu, J., Emilsson, V., 2013. Integrated systems approach identifies genetic nodes and networks in late-onset Alzheimer's disease. Cell 153, 707–720.
Zhu, Y., Nwabuisi-Heath, E., Dumanis, S.B., Tai, L.M., Yu, C., Rebeck, G.W., LaDu, M.J., 2012. APOE genotype alters glial activation and loss of synaptic markers in mice. Glia 60, 559–569.